

## CHAPTER 16

### APPLICATION OF WAVE DIFFRACTION DATA

Richard Sylvester<sup>(1)</sup> and Teck-Kong Lim<sup>(2)</sup>

#### ABSTRACT

By considering separately the two terms of the Sommerfeld solution of wave diffraction behind a semi-infinite breakwater, the influence of the wave reflection from the structure can be evaluated. The diffraction coefficient at any point can be obtained from a graph or table for full, partial or no reflection by the simple addition of two coefficients. From the similarity of the energy-spreading process to the dam-burst problem, it was found that wave heights decreased consistently along the near circular crests for all distances from the breakwater tip. For a workable range of incident angle and distance from the breakwater, wave heights could be defined by this arc distance from the shadow line expressed in wave lengths. These relationships have been verified experimentally for all but the smallest incident angle in proximity to the breakwater. This can be likened to the dam model in which the dam is moving too slowly to permit normal spreading.

The several theoretical solutions for the breakwater gap, when graphed on the same basis, are shown to be very similar, diverging only for small incident angles. New parameters are provided which greatly simplify the presentation of information. The scatter of past experimental data precludes the verification of this theory and indicates the need for further tests.

#### INTRODUCTION

Theoretical solutions have been available over many years for computing wave heights behind breakwaters. These are based upon the diffraction process in optics and hence have given rise to the term "shadow zone" for the area behind the structure. The relevant equations can be solved by computer and thus results, to apparent high degrees of precision, are becoming available. This tendency perhaps is not commensurate with the inaccuracies inherent in the wave data of coastal engineering problems.

This paper attempts to simplify the presentation of information by an averaging process, thus reducing the number of variables. The modest error so introduced should not influence the accuracy of general design procedures.

---

(1) Professor of Coastal Engineering, Asian Institute of Technology,  
Bangkok, Thailand.

(2) Graduate Student, AIT, Bangkok, Thailand

Diffracti<sup>n</sup> of ocean waves can be divided to three main topics, namely: (a) the semi-infinite breakwater, in which the water zone beyond the breakwater is considered to be unlimited as far as wave energy supply is concerned

(b) the breakwater gap, in which two structures extend to less than five wave lengths apart, so limiting the wave energy available for spreading into the one or two shadow zones so formed

(c) the island or offshore breakwater, in which waves diffract to leeward of the structure from either end

Only cases (a) & (b) are discussed in this paper, with the following assumptions applying: (1) uniform depth of water throughout, inferring a constant wave length for any specific wave period

(ii) breakwaters which have a width that can be considered thin in respect to the wave length If the structure or land mass has a sizable width the diffraction solution should be applied from the leeward or shadow-zone face.

(iii) small amplitude waves in keeping with the linear theory, although experimental verification is available for relatively steep waves

#### SEMI-INFINITE BREAKWATER

The general case is illustrated in Figure 1 in which it is seen that a train of waves is approaching at an angle  $\theta$  to the breakwater Thus the orthogonals of the incident waves are angled  $\theta$  to the structure and the one passing through the breakwater tip will be considered the limit of the shadow zone and will be termed the "shadow line". Wave heights only in the shadow zone are considered in this paper. The location of any point P will be defined by either the polar coordinate system ( $\alpha$ , R/L) or the circular arc system (S/L, R/L) As will be seen later, this latter system can be reduced to S/L alone, with little loss of accuracy.

It can also be observed in Figure 1 that the waves reflected from the breakwater also diffract whilst they proceed seawards Before entering the shadow zone they must spread through an angle of  $360^\circ - 2\theta$ , so that to supply energy at point P they have a diffraction angle of  $360^\circ - 2\theta + \alpha$  Outside the shadow zone the interaction of the reflected waves with the incident waves creates a short-crested system, the detailed characteristics of which are available<sup>(1)</sup> Immediately outside the shadow zone the two waves are practically aligned and, although a slight phase difference may be present between the incident and the reflected waves, heights in excess of those of the incident wave are theoretically possible As noted already, this zone is not treated herein

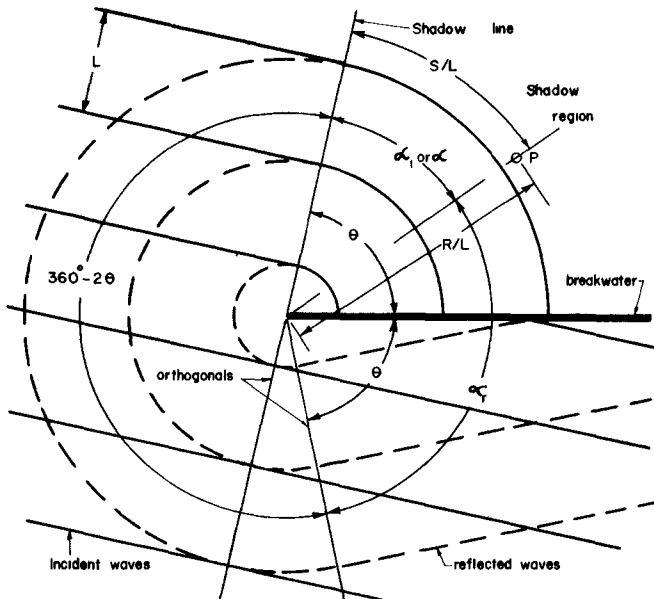


FIG 1  
DEFINITION  
SKETCH

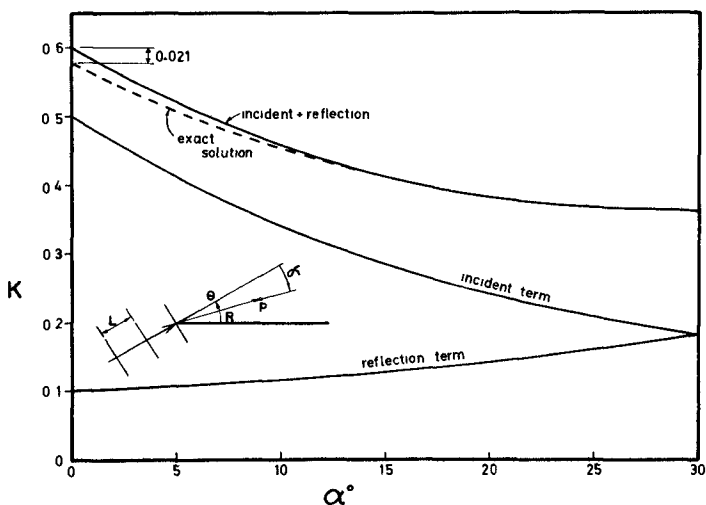


FIG 2  
COMPARISON  
OF METHODS  
FOR  $R/L = 2.5$   
AND  $\theta \approx 30^\circ$

It can be readily accepted that the influence of the reflected wave in the shadow zone is small, but no insignificant for the case of 100% reflection. Inspite of the tendency to design breakwaters for the fullest dissipation of waves, diffraction theory in current use is based upon 100% reflection. In proximity to the breakwater tip, where the reflection component is greatest its correct assessment could result in worthwhile economies of design.

## THEORETICAL SOLUTION

The Sommerfeld<sup>(2)</sup> solution of optical diffraction was applied to water waves by Penney and Price<sup>(3)(4)</sup>. The basic equation with the definition of  $\alpha_1$  and  $\alpha_r$  as in Figure 1, can be written as follows:

$$F(R,\alpha) = f(u_1) \cdot \exp(-ikR \cos \alpha_1) + f(u_2) \cdot \exp(-ikR \cos \alpha_r) \quad \dots \quad (1)$$

$$\text{where } u_1 = -\sqrt{8R/L} \sin(\alpha_1/2) \quad \dots \dots \dots \quad (2)$$

$$f(-u) = \frac{1+i}{2} \int_{-\infty}^0 e^{(1-i)\frac{u}{2}} \exp(-\frac{1}{2}u^2) du \quad \dots \dots \dots (6)$$

$$f(u) + f(-u) = 1 \quad \text{for } u \in \mathbb{R} \quad (7)$$

The diffraction coefficient  $K$  is defined as

$$K = \frac{\text{diffracted wave height}}{\text{incident wave height}} \quad \dots \dots \dots \quad (8)$$

In this event the second term of the RHS in equation (1) can be written  $f(u_2) \exp(-ikR \cos 360^\circ - \alpha_r)$  ..... . .... (10)  
 which represents the diffraction of the reflected wave, from its orthogonal through the breakwater tip around to the polar direction of point P. The first term of equation (1) represents the fraction of the wave height resulting from diffraction of the incident wave from the shadow line. Thus

$$K = |F(R.\alpha)| = \text{incident term} + \text{reflected term.}$$

The generalised form for equation (9) is thus

$$K = \left| f(u) \exp(-i k R \cos \alpha) \right| \dots \dots \dots \quad (11)$$

in which  $\alpha$  can be measured from the shadow line to give the diffraction coefficient for the incident wave, and from the tip orthogonal of the reflected wave ( $360 - 2\theta + \alpha$ ) to give the coefficient for the reflection component. The two values are added to give K for the case of 100% reflection. For partial reflection a proportion of the second component should be used.

Separating the components in the above manner introduces a slight error for incident angles  $\theta \leq 45^\circ$ , but this is on the conservative side and it occurs only near the shadow line and for small radial distances as indicated in Figure 2.

Larras<sup>(5)</sup> has recently made a similar approach to the problem, by solving the sine and Fresnel functions from the geometry of the point P in terms of orthogonal axes and the use of Cornu spirals. In this case also the diffraction coefficient is the addition of an incident and reflected term, the latter being modified according to the degree of reflection.

#### POLAR CO-ORDINATE SYSTEM

Equation (11) can be graphed as in Figure 3, or tabulated as in Table I. The values of K representing incident and reflected components are read from the angle  $\alpha$  as previously indicated and then added. For example, with  $\theta = 60^\circ$ ,  $\alpha = 30^\circ$  and  $R/L = 10$  we have from Figure 3:  $360 - 2(60) + 30 = 270^\circ$ , so that  $K(\text{incident}) = 0.10$  and  $K(\text{reflected}) = 0.03$ , giving  $K(\text{100\% reflection}) = 0.13$ ,  $K(\text{zero reflection}) = 0.10$  and  $K(\text{50\% reflection}) = 0.115$ .

The respective values as obtained from Table I are as follows:

$$\begin{aligned} K(\alpha = 30^\circ) &= 0.096 \\ K(360^\circ - 2\theta + \alpha = 270^\circ) &= K(360^\circ - 270^\circ = 90^\circ) = 0.036 \\ K(\text{100\% reflection}) &= 0.132 \end{aligned}$$

In reading table I it is sufficient for the reflection term to use  $2\theta - \alpha$ , which in this case =  $120^\circ - 30^\circ = 90^\circ$ .

It is noteworthy that with no reflection the wave height along the shadow line ( $\alpha = 0^\circ$ ) remains static at 0.5. Also, on the lee-side of the breakwater, where  $\alpha = \theta$ , it is found that the incident and reflection components are each 50% of the total. This is significant when the latter might not exist at all due to adequate dissipation on the breakwater.

#### CIRCULAR ARC SYSTEM

Consider the wave at the shadow line just after it has reached the the breakwater. At the crest alignment two distinct water levels attempt to exist simultaneously, that of the wave crest and that of the still-water level inside the shadow zone. This instantaneous

TABLE 1 -  $K' = |f(u) \exp(-2\pi i(R/L)\cos(\alpha))|$ 

$\alpha$ degrees	R/L	K' x 1/1000									
		1	2	3	4	5	6	8	10	15	20
0	500	500	500	500	500	500	500	500	500	500	500
2	476	466	459	453	448	443	435	428	413	402	
4	453	435	422	411	402	393	379	367	344	325	
6	431	406	388	373	361	350	332	317	288	266	
8	411	379	357	340	325	313	292	275	244	222	
10	392	355	329	310	294	280	258	241	210	188	
12	373	332	304	283	267	253	230	213	182	162	
14	356	311	282	260	243	229	207	190	161	141	
16	340	292	262	240	222	208	187	170	143	125	
18	325	275	244	221	204	191	170	154	128	112	
20	310	259	228	205	189	175	155	140	116	101	
25	278	225	194	173	157	145	127	115	94	82	
30	251	197	168	148	134	123	107	96	79	69	
35	228	175	147	129	116	107	93	83	68	59	
40	208	157	131	115	103	94	82	73	60	52	
45	191	142	118	103	92	84	73	66	54	46	
50	176	130	107	93	84	77	66	59	49	42	
55	164	120	99	86	77	70	61	54	44	39	
60	153	111	91	79	71	65	56	50	41	36	
65	143	104	85	74	66	60	52	47	38	33	
70	135	97	80	69	62	57	49	44	36	31	
75	128	92	75	65	58	53	46	41	34	29	
80	122	87	71	62	55	51	44	39	32	28	
85	116	83	68	59	53	48	42	37	30	26	
90	111	79	65	56	50	46	40	36	29	25	
95	107	76	62	54	48	44	38	34	28	24	
100	103	73	60	52	46	42	37	33	27	23	
105	99	71	58	50	45	41	35	32	26	22	
110	96	69	56	49	43	40	34	31	25	22	
115	94	67	54	47	42	39	33	30	24	21	
120	91	65	53	46	41	38	32	29	24	21	
125	89	63	52	45	40	37	32	28	23	20	
130	87	62	51	44	39	36	31	28	23	20	
135	86	61	50	43	39	35	30	27	22	19	
140	84	60	49	42	38	35	30	27	22	19	
145	83	59	48	42	37	34	29	26	22	19	
150	82	58	48	41	37	34	29	26	21	18	
160	80	57	47	40	36	33	29	26	21	18	
170	80	56	46	40	36	33	28	25	21	18	
180	79	56	46	40	36	32	28	25	21	18	

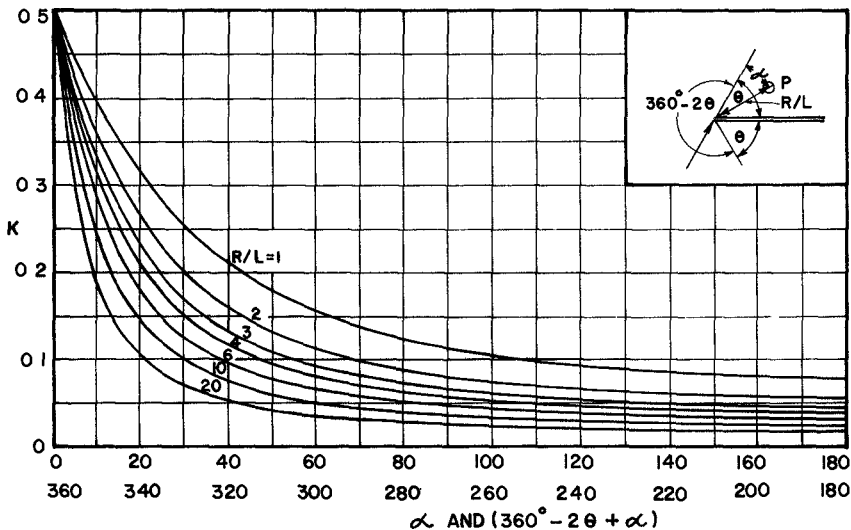
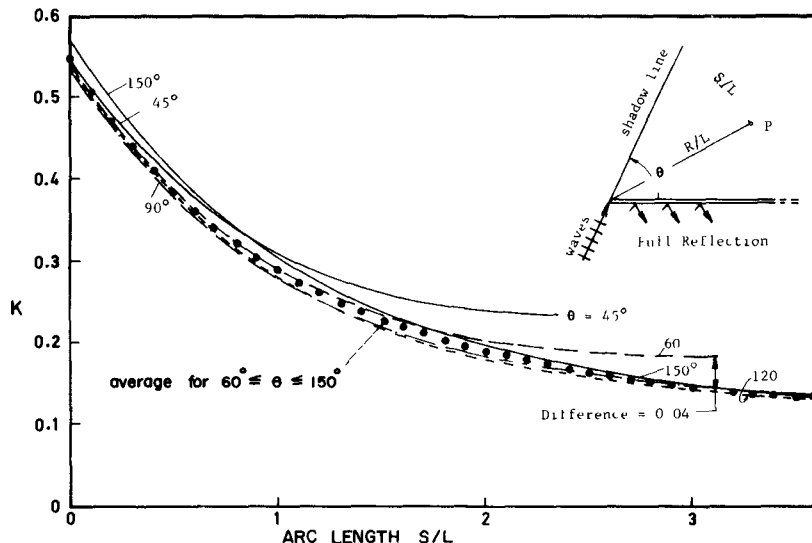
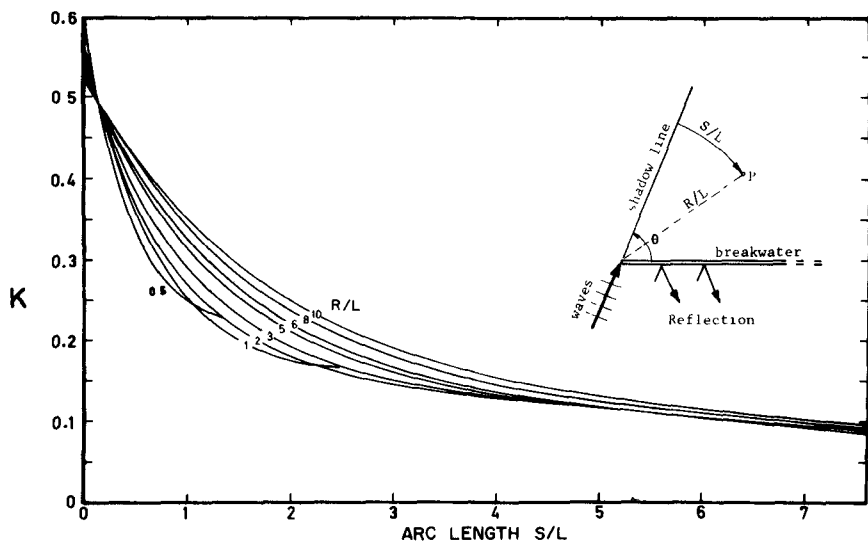


FIG.3 K FOR ALL  $\theta$  WITH OR WITHOUT REFLECTION

differential can be likened to the dam-break problem, in which the vertical wall of water gives way to a sloping surface which flattens swiftly with time

The major differences in these two phenomena are the element of time and the supply of energy. In the case of the dam-burst the slope at the channel alignment varies with time, whereas in diffraction the wave crest is changing position and would appear to maintain a fixed profile. In respect to energy supply, this is limited in the dam case by the volume of water available in the reservoir, but appears unlimited for the semi-infinite length of the wave crests outside the shadow zone of the breakwater. This comparison suffers many disabilities, but it is felt significant that the water at the dam site remains constant at  $4/9$  of the original depth, whilst the energy level remains constant. In an apparently similar manner the energy transfer in diffraction, for the incident wave alone, maintains a constant depth along the shadow line. The order of the depth changes are vastly different and crest to trough measurements are involved rather than SWL, so that strict equality cannot be expected.

From the above generalisations it was surmised that along a wave crest, which in the shadow zone could be accepted as circular in plan, a constant wave-height profile should exist for all its positions from the breakwater. This distance measurement from the shadow line is designated an arc length ( $S/L$ ) which could thus replace the  $(R/L, \alpha)$  coordinate system previously used for defining positions in the shadow zone. (See Figure 1).

FIG 4 K VALUES FOR  $R/L = 3$  AND FULL REFLECTION.FIG 5 K AVERAGED FOR  $60^\circ \leq \theta \leq 150^\circ$  AND FULL REFLECTION

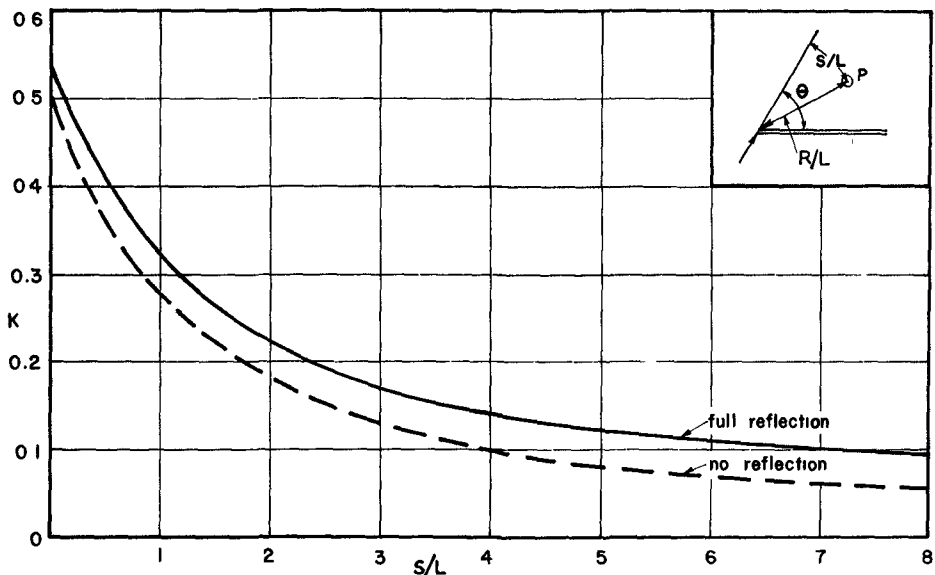


FIG 6 K ALONG CREST FOR  $60^\circ \leq \theta \leq 150^\circ$  AND  $3 \leq R/L \leq 10$

Curves were drawn from the Sommerfeld solution in the circular arc system for values of  $R/L = 0.5$  to  $10$  and  $\theta = 45^\circ$  to  $180^\circ$ . A typical set of results is displayed in Figure 4, which shows the curves for the various angles  $\theta$  and the specific value of  $R/L = 3$ . An average curve was drawn for  $\theta = 60^\circ$  to  $150^\circ$ , as indicated, for each  $R/L$  value and then collected in a single diagram (as Figure 5). From this a single curve appeared acceptable to represent  $R/L$  values from 3 to 10.

The errors so introduced by this averaging procedure can be ascertained from the two figures. As seen in Figure 4, that due to averaging  $\theta$  occurs mainly in the smaller  $\theta$  values, for example a maximum of  $K = +0.04$  for  $\theta = 60^\circ$  at  $S/L = 3$  for the case of  $R/L = 3.0$ . In Figure 5 an average line (not drawn) involves a maximum error of about  $\pm 0.035$  at  $S/L = 2.0$ , or 3.5% of the incident wave. These error values are not strictly cumulative since they occur at different  $S/L$  values and the first one quoted is for the  $60^\circ$  incident angle only. The average error for  $\theta$  larger than this was in the order of  $\pm 0.01$ .

Figures 4 and 5 represent full reflection conditions. Similar graphs can be obtained for zero reflection, resulting in the curves of Figure 6. This figure can be used instead of Figure 3 or Table I with

the slight loss of accuracy indicated To find the relevant S/L value an arc should be drawn through the point of interest P, centered on the breakwater tip, and the length along it from the shadow line measured in wave lengths. This can be accomplished on any harbour layout where constant depths can be assumed

#### EXPERIMENTAL VERIFICATION

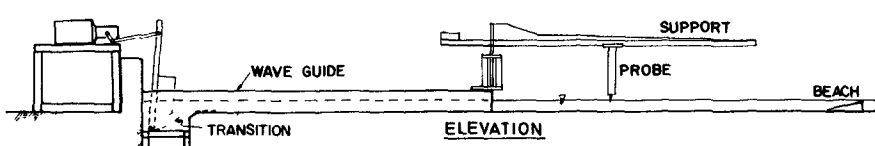
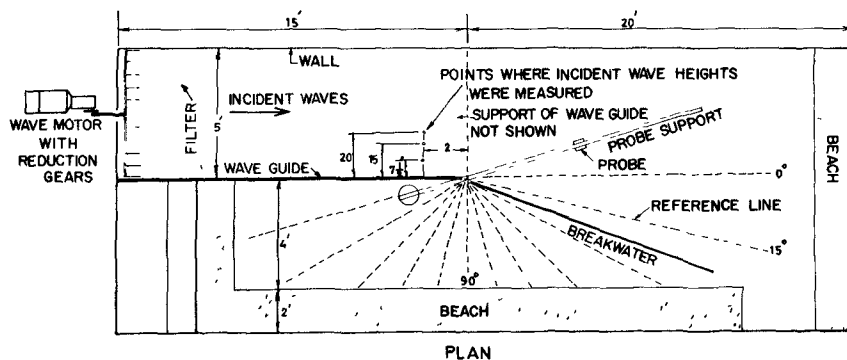
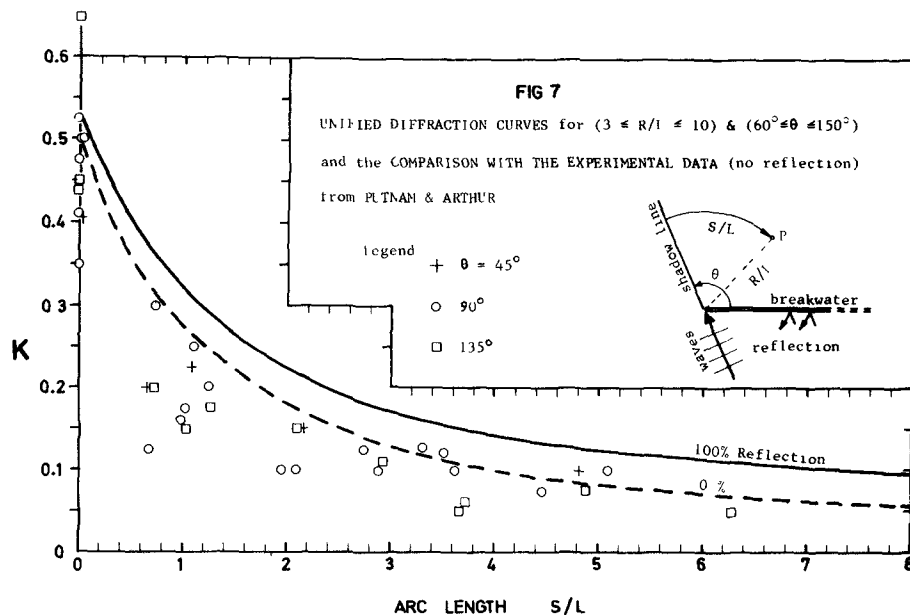
Putman and Arthur<sup>(6)</sup> conducted experiments which avoided reflection from the breakwater Their results, which were presented in x-y coordinates, were transformed to the arc length system and are displayed in Figure 7 Agreement is clearly shown with the zero reflection curve.

Tests conducted by Lim<sup>(7)</sup> at the Asian Institute of Technology were concentrated on the region within three wave lengths of the breakwater tip Incident angles of 45°, 60°, 90°, 120° and 180° were examined and measurements were made for R/L = 1, 2 and 3 at intervals of either 7½° or 15° from the shadow line The main elements of the equipment are shown in Figure 8, where it is seen that the incident angles were varied by changing the position of the breakwater. Reflection from the exposed side of the breakwater is obviously excluded.

Waves were measured by a step wave probe to an accuracy of  $\pm 1.0$  mm. The range of wave heights and wave periods for all tests are listed in Table II where it can be noted that periods ranged from 0.5 to 0.7 seconds and incident wave heights from 19 to 36 mm This latter measurement was an average of values taken at 3 points in the approach channel (See Figure 8) to obviate the resonant cross-waves established there.

Results from runs with similar waves presented some scatter, as exemplified in Figures 9 and 10 and observed in Table II. This would have arisen from the probe error, incomplete dissipation of the waves at the basin boundary, and long period surge of the basin Averages of the several runs are listed in Table II for each  $\alpha$  and R/L value (probe location), and graphed for each  $\theta$  in Figures (11 to 15). For angles of 60° and 90° the experimental data agree very well with the theory for zero reflection. For angles 120° and 180° the experimental points are a little low, but for 45° are high, in all cases increasing with distance inside the shadow zone. This difference decreased as R/L approached 3. The maximum error was in the order of 4% of the incident wave height. Since the theory is conservative for  $\theta \geq 60^\circ$ , based upon this experimental evidence, it is suggested that Figures 3 and 6 or Table I can be used with confidence, by computing an appropriate allowance for reflection.

For the special conditions of  $\theta < 60^\circ$  and  $R/L < 3$ , an addition of 0.1 should be made to the K evaluated above The previous comparison of wave diffraction to the dam-burst problem may help explain this deviation from the theory. When  $\theta$  is small the wave has insufficient room to spread properly. This situation is similar to a moving dam whose velocity does not permit the formation of the water surface profile commensurate with a sudden dam collapse

**FIG 8 TEST EQUIPMENT**

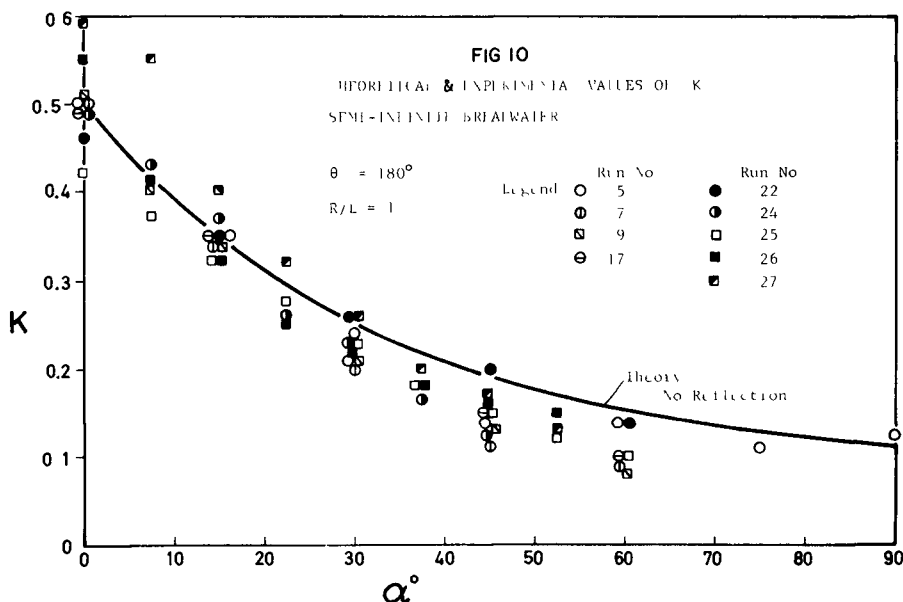
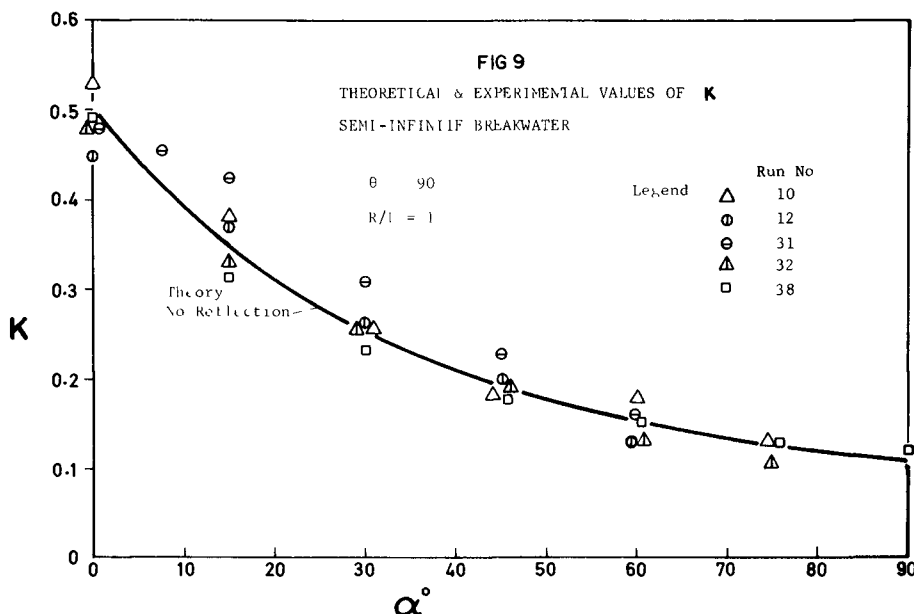
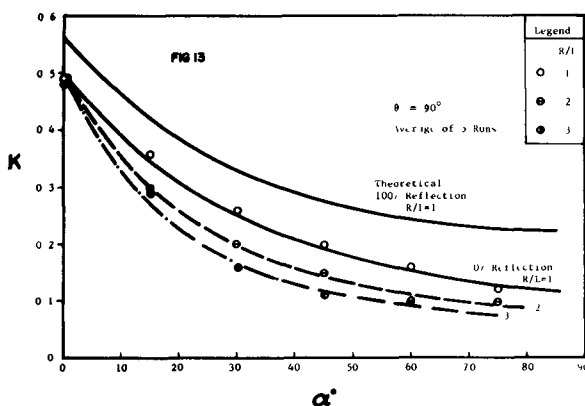
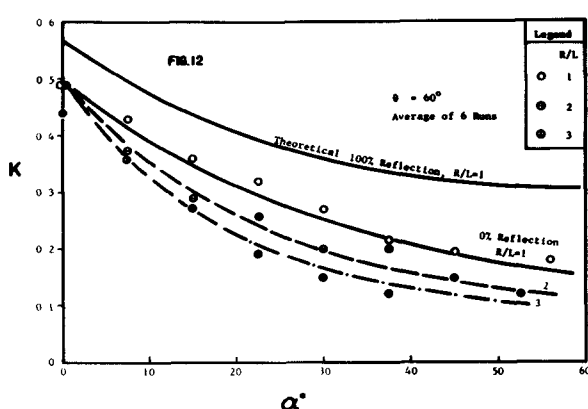
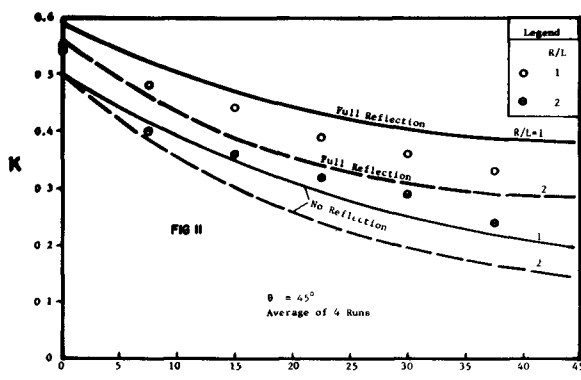
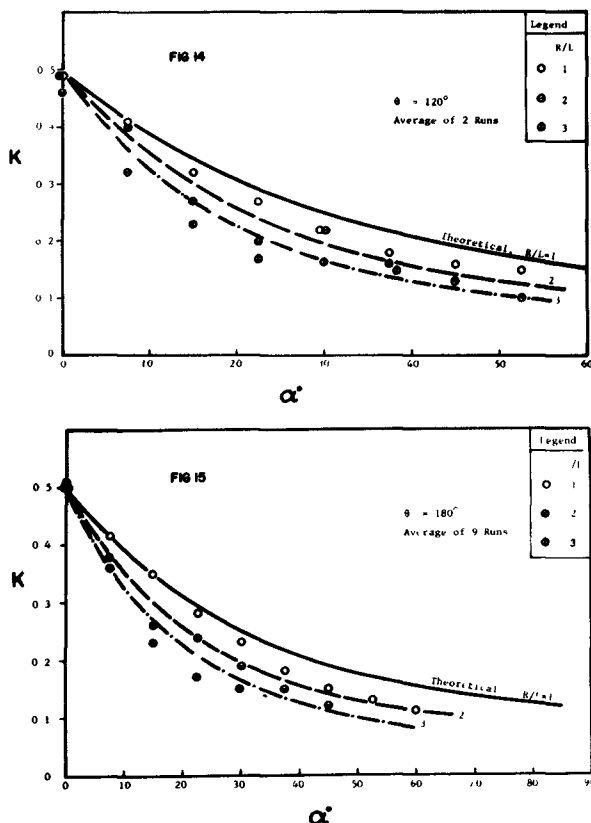


Table II. Results of Experiments in Semi-infinite Breakwater With No Reflections

E <sub>L</sub>	H <sub>L</sub>	EXPERIMENTAL E					THEORETICAL E					EXPERIMENTAL E					THEORETICAL E					
		10	19	20	37	Average	10	19	20	37	Average	10	19	20	37	Average	10	19	20	37	Average	
$\theta = 45^\circ$																						
1	0	56	52	64	49	55	569	500	569	500	569	1	7	5	56	46	49	51	49	51	500	
1.5	42	45	49	43	44	44	545	545	545	545	545	1.5	12	12	42	35	35	35	35	35	500	
2	22	23	26	29	42	41	39	449	500	500	500	500	2	7	5	56	46	49	51	49	500	
2.5	20	25	29	27	34	36	402	231	231	231	231	2.5	12	12	42	35	35	35	35	35	500	
3	7	10	12	16	26	25	35	329	329	329	329	329	3	12	12	42	35	35	35	35	35	
4	0	13	27	35	39	36	561	500	500	500	500	4	12	12	42	35	35	35	35	35	500	
5	7.5	12	13	15	22	22	56	500	500	500	500	500	5	12	12	42	35	35	35	35	35	500
6	22	23	26	30	40	31	32	569	500	500	500	500	6	12	12	42	35	35	35	35	35	500
7	15	20	23	26	32	25	35	500	500	500	500	500	7	12	12	42	35	35	35	35	35	500
8	15	20	23	26	32	25	35	500	500	500	500	500	8	12	12	42	35	35	35	35	35	500
9	0	48	59	61	56	46	549	500	500	500	500	9	12	12	42	35	35	35	35	35	500	
10	22	23	26	30	31	26	35	500	500	500	500	500	10	12	12	42	35	35	35	35	35	500
11	22	23	26	30	31	26	35	500	500	500	500	500	11	12	12	42	35	35	35	35	35	500
12	22	23	26	30	31	26	35	500	500	500	500	500	12	12	12	42	35	35	35	35	35	500
13	22	23	26	30	31	26	35	500	500	500	500	500	13	12	12	42	35	35	35	35	35	500
14	22	23	26	30	31	26	35	500	500	500	500	500	14	12	12	42	35	35	35	35	35	500
15	22	23	26	30	31	26	35	500	500	500	500	500	15	12	12	42	35	35	35	35	35	500
16	22	23	26	30	31	26	35	500	500	500	500	500	16	12	12	42	35	35	35	35	35	500
17	22	23	26	30	31	26	35	500	500	500	500	500	17	12	12	42	35	35	35	35	35	500
18	22	23	26	30	31	26	35	500	500	500	500	500	18	12	12	42	35	35	35	35	35	500
19	0	19	3	23	7	19	7	500	500	500	500	500	19	12	12	42	35	35	35	35	35	500
20	0	19	3	23	7	19	7	500	500	500	500	500	20	12	12	42	35	35	35	35	35	500
21	0	19	3	23	7	19	7	500	500	500	500	500	21	12	12	42	35	35	35	35	35	500
22	0	19	3	23	7	19	7	500	500	500	500	500	22	12	12	42	35	35	35	35	35	500
23	0	19	3	23	7	19	7	500	500	500	500	500	23	12	12	42	35	35	35	35	35	500
24	0	19	3	23	7	19	7	500	500	500	500	500	24	12	12	42	35	35	35	35	35	500
25	0	19	3	23	7	19	7	500	500	500	500	500	25	12	12	42	35	35	35	35	35	500
26	0	19	3	23	7	19	7	500	500	500	500	500	26	12	12	42	35	35	35	35	35	500
27	0	19	3	23	7	19	7	500	500	500	500	500	27	12	12	42	35	35	35	35	35	500
28	0	19	3	23	7	19	7	500	500	500	500	500	28	12	12	42	35	35	35	35	35	500
29	0	19	3	23	7	19	7	500	500	500	500	500	29	12	12	42	35	35	35	35	35	500
30	0	19	3	23	7	19	7	500	500	500	500	500	30	12	12	42	35	35	35	35	35	500
31	0	19	3	23	7	19	7	500	500	500	500	500	31	12	12	42	35	35	35	35	35	500
32	0	19	3	23	7	19	7	500	500	500	500	500	32	12	12	42	35	35	35	35	35	500
33	0	19	3	23	7	19	7	500	500	500	500	500	33	12	12	42	35	35	35	35	35	500
34	0	19	3	23	7	19	7	500	500	500	500	500	34	12	12	42	35	35	35	35	35	500
35	0	19	3	23	7	19	7	500	500	500	500	500	35	12	12	42	35	35	35	35	35	500
36	0	19	3	23	7	19	7	500	500	500	500	500	36	12	12	42	35	35	35	35	35	500
37	0	19	3	23	7	19	7	500	500	500	500	500	37	12	12	42	35	35	35	35	35	500
38	0	19	3	23	7	19	7	500	500	500	500	500	38	12	12	42	35	35	35	35	35	500
39	0	19	3	23	7	19	7	500	500	500	500	500	39	12	12	42	35	35	35	35	35	500
40	0	19	3	23	7	19	7	500	500	500	500	500	40	12	12	42	35	35	35	35	35	500
41	0	19	3	23	7	19	7	500	500	500	500	500	41	12	12	42	35	35	35	35	35	500
42	0	19	3	23	7	19	7	500	500	500	500	500	42	12	12	42	35	35	35	35	35	500
43	0	19	3	23	7	19	7	500	500	500	500	500	43	12	12	42	35	35	35	35	35	500
44	0	19	3	23	7	19	7	500	500	500	500	500	44	12	12	42	35	35	35	35	35	500
45	0	19	3	23	7	19	7	500	500	500	500	500	45	12	12	42	35	35	35	35	35	500
46	0	19	3	23	7	19	7	500	500	500	500	500	46	12	12	42	35	35	35	35	35	500
47	0	19	3	23	7	19	7	500	500	500	500	500	47	12	12	42	35	35	35	35	35	500
48	0	19	3	23	7	19	7	500	500	500	500	500	48	12	12	42	35	35	35	35	35	500
49	0	19	3	23	7	19	7	500	500	500	500	500	49	12	12	42	35	35	35	35	35	500
50	0	19	3	23	7	19	7	500	500	500	500	500	50	12	12	42	35	35	35	35	35	500
51	0	19	3	23	7	19	7	500	500	500	500	500	51	12	12	42	35	35	35	35	35	500
52	0	19	3	23	7	19	7	500	500	500	500	500	52	12	12	42	35	35	35	35	35	500
53	0	19	3	23	7	19	7	500	500	500	500	500	53	12	12	42	35	35	35	35	35	500
54	0	19	3	23	7	19	7	500	500	500	500	500	54	12	12	42	35	35	35	35	35	500
55	0	19	3	23	7	19	7	500	500	500	500	500	55	12	12	42	35	35	35	35	35	500
56	0	19	3	23	7	19	7	500	500	500	500	500	56	12	12	42	35	35	35	35	35	500
57	0	19	3	23	7	19	7	500	500	500	500	500	57	12	12	42	35	35	35	35	35	500
58	0	19	3	23	7	19	7	500	500	500	500	500	58	12	12	42	35	35	35	35	35	500
59	0	19	3	23	7	19	7	500	500	500	500	500	59	12	12	42	35	35	35	35	35	500
60	0	19	3	23	7	19	7	500	500	500	500	500	60	12	12	42	35	35	35	35	35	500
61	0	19	3	23	7	19	7	500	500	500	500	500	61	12	12	42	35	35	35	35	35	500
62	0	19	3	23	7	19	7	500	500	500	500	500	62	12	12	42	35	35	35	35	35	500
63	0	19	3	23	7	19	7	500	500	500	500	500	63	12	12	42	35	35	35	35	35	500
64	0	19	3	23	7	19	7	500	500	500	500	500	64	12	12	42	35	35	35	35	35	500
65	0	19	3	23	7	19	7	500	500	500	500	500	65	12	12	42	35	35	35	35	35	500
66</																						



FIGS 11, 12, 13. THEORETICAL AND EXPERIMENTAL VALUES OF OIF-FRACTION COEFFICIENT (K), SEMI-INFINITE BREAKWATER, NO REFLECTION



FIGS 14, 15. THEORETICAL AND EXPERIMENTAL VALUES OF DIFFRACTION COEFFICIENT ( $K$ ), SEMI-INFINITE BREAKWATER, NO REFLECTION

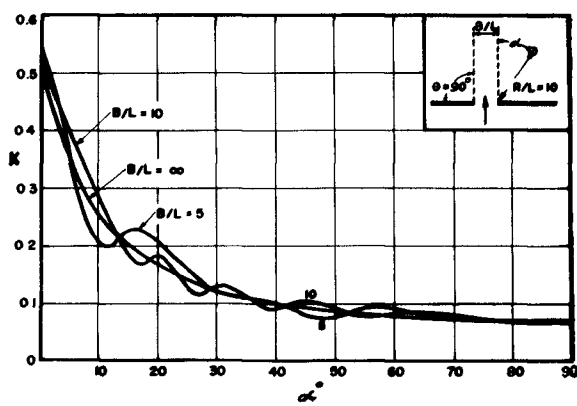


FIG 16. INFLUENCE OF GAP WIDTH ON DIFFRACTION COEFFICIENT

## BREAKWATER GAP

Where two breakwaters are aligned and full reflection is realised from each, the waves in each shadow zone are comprised of the incident wave and the two reflected waves. Since the crest curvature of one of these is not centered on the breakwater tip of the incident and other reflected wave, the resultant wave height measured along the arc length fluctuates about the smooth curve of the semi-infinite breakwater solution. This is illustrated in Figure 16, where it can be observed that the deviations increase as the gap width decreases. Down to the value of  $B/L = 5$  the semi-infinite breakwater solution can be used without great loss of accuracy. Where no reflection occurs such undulations are not present as noted in the experiments reported herein, which are essentially half a breakwater gap without the reflection component.

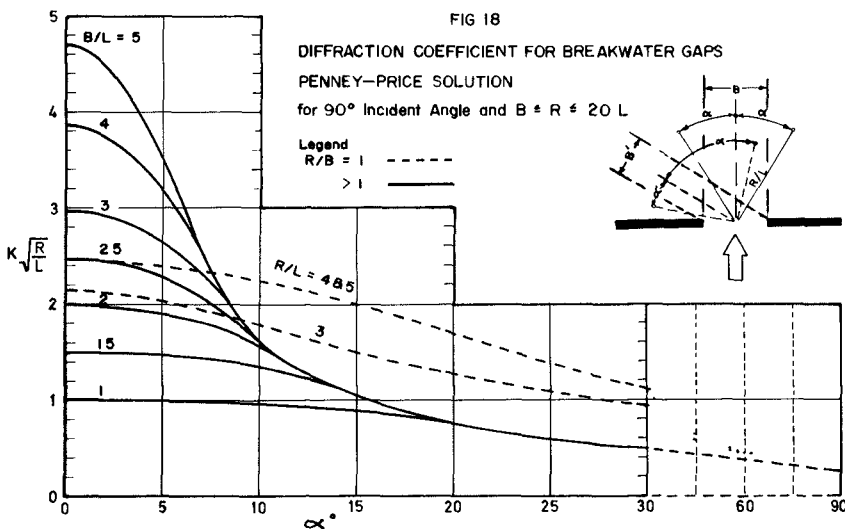
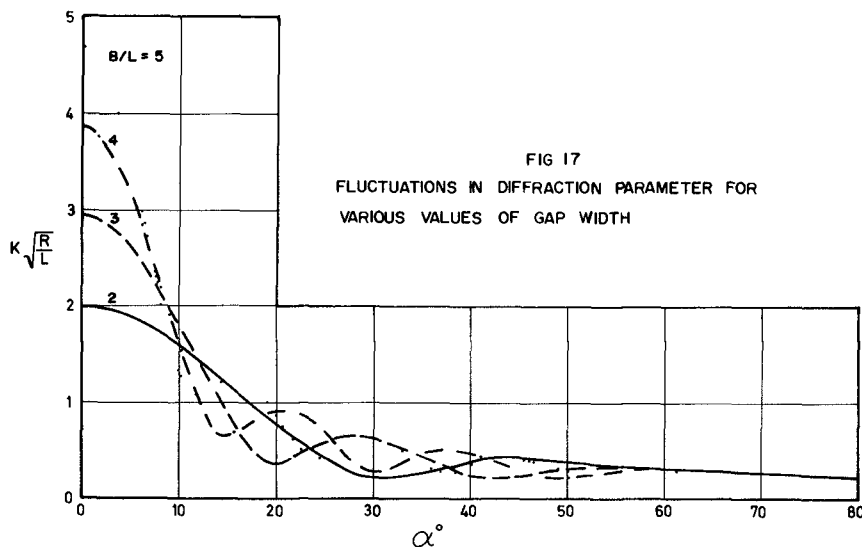
APPLICATION OF SOMMERFELD'S SOLUTION<sup>(4)</sup>

It can be shown, by graphing values of  $K$  and  $R/L$  in Table I, that the wave height is reduced in proportion to  $(R/L)^{1/2}$ . This suggests a parameter  $K\sqrt{R/L}$  for combining radial and arc distance influences. It is also convenient to centre the polar coordinate at the mid-point of the breakwater gap. In the knowledge that for  $R > 5B$  the value of  $K\sqrt{R/L}$  is essentially constant for any  $\alpha$  a simple series of graphs can represent conditions anywhere in the protected basin. An example of this is Figure 17, which is drawn for  $R/L = 20$ , the largest probable radius to be encompassed. In the absence of reflection, the fluctuations exhibited in Figure 17 will not be present, so that averaging them should not involve undue error in a prototype situation. Figure 18 results for  $\theta = 90^\circ$  and  $B/L \leq R/L \leq 20$ , in which curves are grouped into two categories:  $R/B = 1$  and  $R/B > 1$ . For gaps smaller than  $2L$  the single curve (full line) represents both cases of  $R/B$ .

The above simplifications lead to a maximum error in  $K\sqrt{R/L}$  of  $\pm 0.3$  at the maxima and minima of the undulations (See Figure 17). The average deviation is in the order of  $\pm 0.2$ . Since reflection is likely to be much smaller than 100% these errors appear acceptable. Although Figure 18 applies only to  $\theta = 90^\circ$ , other angles can be treated by the method suggested by Blue and Johnson<sup>(8)(9)</sup>, in which the equivalent width  $B'$  is used for the angle  $\theta$  (See inset of figure).

## MORSE-RUBENSTEIN SOLUTION

For gap widths of  $3L$  and less an exact solution in optics has been derived by Morse and Rubenstein<sup>(10)</sup>, and applied to water waves by Carr and Stelzriede<sup>(11)</sup>, to which the reader is referred for the relevant equations. The computation procedure is tedious, but a graphical solution is provided in Reference No (11).



Using the previously derived parameter  $K\sqrt{R/L}$ , graphs for  $B/L = 0.5, 1.0$  and  $2.0$  are presented in Figure 19 for incident angles of  $30^\circ, 60^\circ$  and  $90^\circ$ . These are applicable to zones where  $R > B$ .

#### LAGOMBE'S SOLUTION

Lacombe<sup>(12)</sup> has derived an approximate solution which is based upon a polar coordinate system centered on the mid-gap point. It applies to  $R > B$  and is best used to determine the maxima values in the fluctuations previously discussed. For  $B \geq 2L$  the solution is close to that of Morse-Rubenstein.

#### COMPARISON OF SOLUTIONS

For the smaller gap widths ( $B \leq 2L$ ) a direct comparison of the above mentioned solutions is possible. As seen in Figures 20 and 21 the solution of Penney and Price<sup>(4)</sup> is extremely close to that of Morse and Rubenstein, for the incident angle of  $90^\circ$  and to the limit of  $\alpha$  to which the latter is carried. For this same normal incidence the Lacombe approximation is sensibly the same. It is not until  $\theta = 30^\circ$  that major deviations occur between the Lacombe and Morse-Rubenstein solutions. The latter should be preferred for design purposes because of its conservative tendencies.

#### EXPERIMENTAL EVIDENCE

Blue<sup>(13)</sup> carried out extensive model tests on diffraction behind a breakwater gap. His measurements were made on a square grid system, which had to be converted to the polar coordinate system. Only those results could be used, therefore, which approximated the  $B/L$  value for the theory. The points plotted in Figures 22 and 23 suffer extreme scatter, which is probably due in part to the variety of depth/wavelength and height/length ratios used, both of which would have influenced the degree of reflection from the vertical walls of the model breakwaters. The results as presented cannot be accepted as verification of the theoretical curves, so that further practical work appears necessary. In order to exclude the reflection component, tests similar to those reported herein are indicated, the only difference being the width of the approach channel in respect to the wave length. No drastic differences in wave attenuation should be expected, since the only change is the limited crest length from which the diffraction energy is supplied.

#### CONCLUSIONS

#### SEMI-INFINITE BREAKWATER

1. The theoretical value of diffraction coefficient for a semi-infinite breakwater can be divided for engineering purposes into two components, arising respectively from the incident and reflected waves.

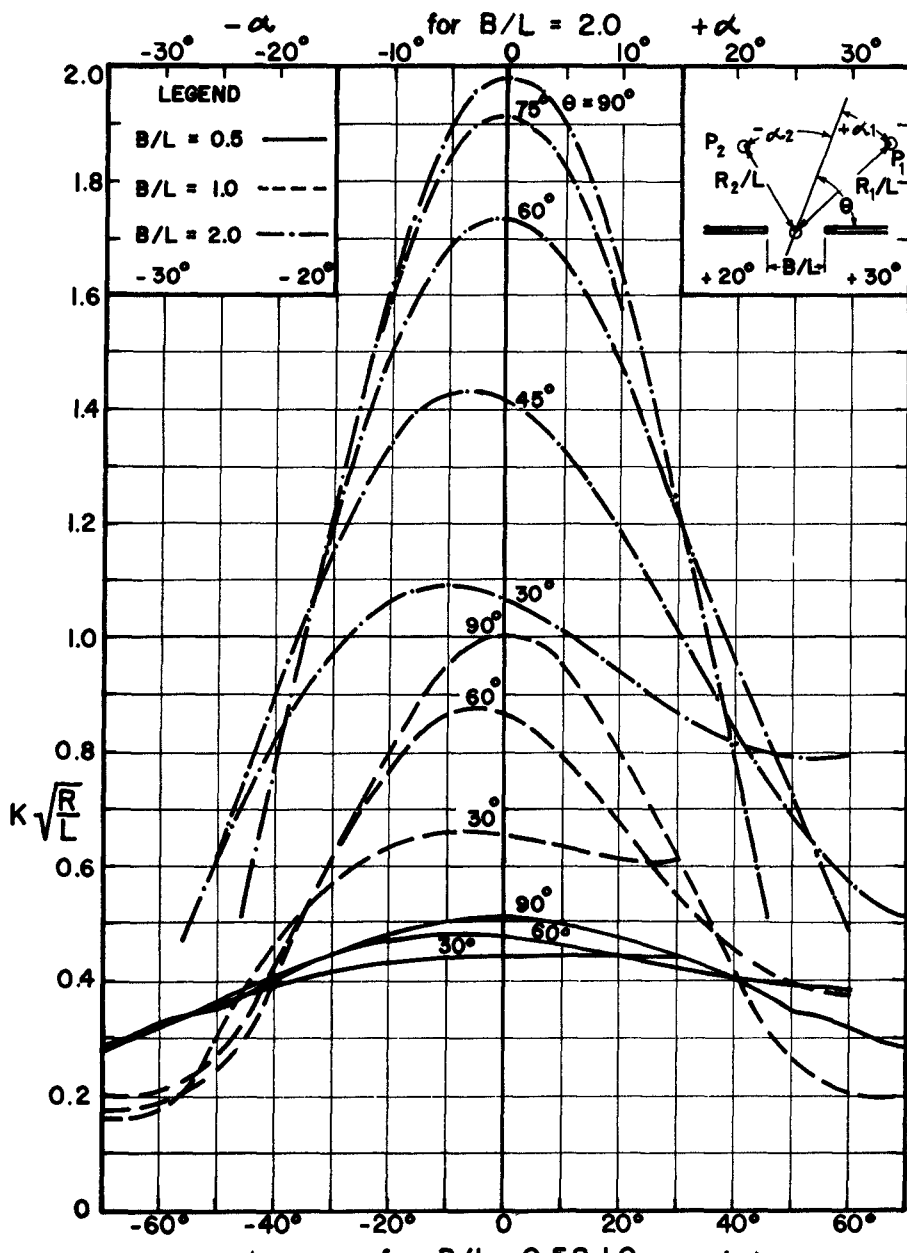
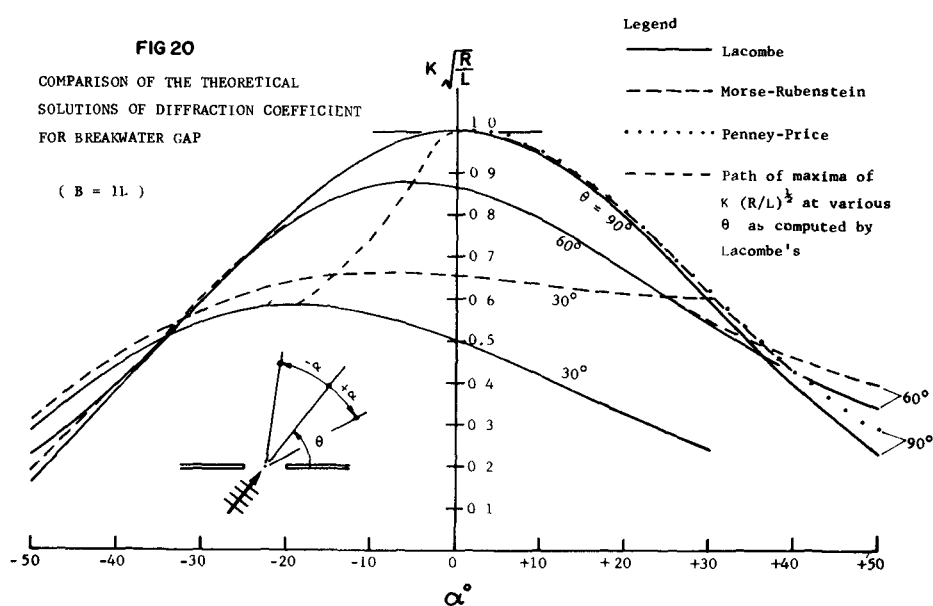


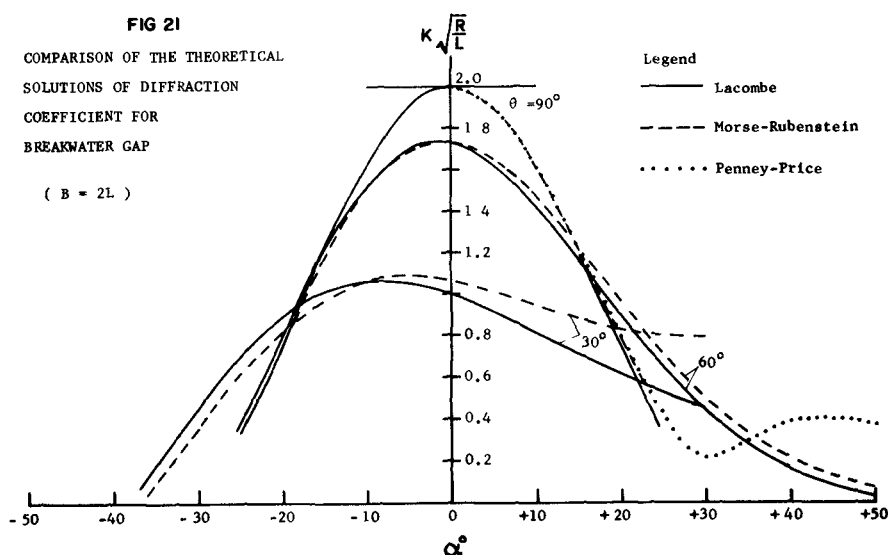
FIG. 19 K FOR B/L = 0.5, 1 & 2 AND  $\theta = 30^\circ, 60^\circ$  &  $90^\circ$

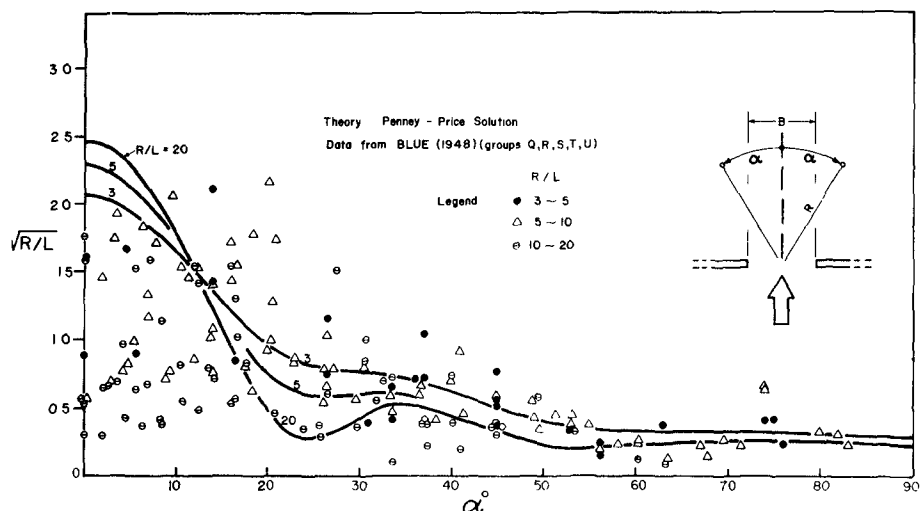
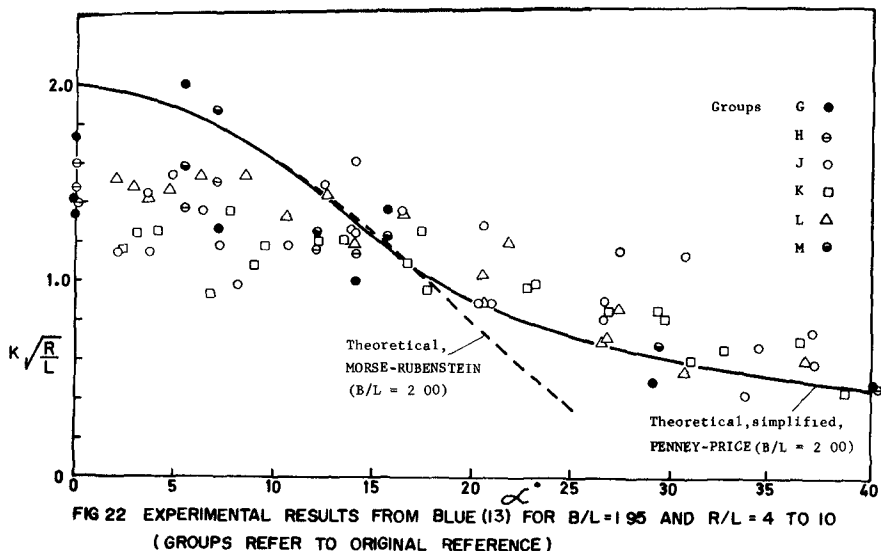
**FIG 20**

COMPARISON OF THE THEORETICAL  
SOLUTIONS OF DIFFRACTION COEFFICIENT  
FOR BREAKWATER GAP

**FIG 21**

COMPARISON OF THE THEORETICAL  
SOLUTIONS OF DIFFRACTION  
COEFFICIENT FOR  
BREAKWATER GAP





2. The diffraction coefficient from (1) above can be presented in a simple table or graph which involves an angular measure and distance from the breakwater tip. The incident and reflection components determined from the angle through which diffraction takes place, are additive.

3. The sensibly constant profile along the nearly circular crests of the diffracting waves permits a simplified presentation of diffraction coefficient for arc distances from the shadow line, which covers a wide range of incidence angle and radial distance. Various degrees of reflection from the breakwater can be incorporated into the diffracted wave height.

4. Experimental evidence confirms the reflection component approach. It also verifies the zero reflection solution for incident angles from  $60^\circ$  to  $150^\circ$  inclusive. For lesser angles an addition of 0.1 in the diffraction coefficient is recommended.

#### BREAKWATER GAP

5. The various theoretical solutions for wave diffraction behind a breakwater gap give very similar results for incident angles approaching  $90^\circ$ . Only when the angle is less than  $45^\circ$  do deviations become pronounced.

6. The simplest presentation of data results from the use of the parameter  $K\sqrt{R/L}$ , together with a polar coordinate system based upon the incident orthogonal passing through the mid-point of the gap.

7. Results from past experiments on the breakwater gap contain too much scatter to verify the theory, indicating the need for further work in this direction.

#### ACKNOWLEDGEMENTS

During the course of this research the junior author was in receipt of a scholarship at the Asian Institute of Technology, formerly the SEATO Graduate School of Engineering. The wave probe was kindly lent by the University of Western Australia, where it was developed by the senior author.

## REFERENCES

- (1) Fan S.H., J.E. Cumming and R.L. Wiegel "Computed Solution of Wave Diffraction by Semi-Infinite Breakwater" University of California, Berkeley, Tech. Rep. HEL-1-8, 1967.
- (2) Sommerfeld A. "Mathematische Theorie der Diffraction" Math. Ann. No.47, 1896, 317-374.
- (3) Penney W.G and Price A.T. "Diffraction of Sea Waves by Breakwaters" Directorate of Miscellaneous Weapons Development. Technical History No.26, Artificial Harbour, Sec.3D.
- (4) Penney W.G and Price A.T. "The Diffraction Theory of Sea Waves by Breakwaters" Phil. Trans. Roy. Soc. (London) A244, 1952, 236-253.
- (5) Larras J. "Diffraction de la Houle par les Obstacles Rectilignes Semi-indefinis sous Incidence Oblique" Cahiers Océanographiques 18, 1966, 661-667.
- (6) Putman J.A. and R.S. Arthur "Diffraction of Water Waves by Breakwaters" Trans Am. Geoph. Un 29, 1948, 481-490.
- (7) Lim T.K. "Wave Diffraction" M.Eng. Thesis, Asian Institute of Technology, Bangkok, Thailand, 1968.
- (8) Blue F.L. and J.W. Johnson "Diffraction of Water Waves Passing Through a Breakwater Gap" Trans. Am Geoph. Un. 30, 1949, 705-718.
- (9) Johnson J.W. "Generalised Wave Diffraction Diagrams" Proc. 2nd Conf. Coastal Eng., 1952, 6-23.
- (10) Morse P.M. and P.J. Rubenstein "The Diffraction of Waves by Ribbons and Slits" Physical Review No.54, 1938, 895-898.
- (11) Carr J.H. and M.E. Stelzriede "Diffraction of Water Waves by Breakwaters" Gravity Waves, U.S. Natl Bur. Stds., Circ. No.521, 1952, 109-125.
- (12) Lacombe H. "The Diffraction of a Swell. A Practical Approximate Solution and its Justification" Gravity Waves, U.S. Natl. Bur. Stds., Circ. No.521, 1952, 129-140.
- (13) Blue F.L. "Diffraction of Water Waves Passing Through a Breakwater Gap" Ph. D. Thesis in Civil Engineering, University of California, Berkeley, 1948